

Supporting Information

Impact of External Short Circuits on Lithium-Ion Batteries: A Post-Mortem Case Study

Shagor Chowdhury,^{*a} Ana Barrera,^a Maya Marinova,^b Alexandre Fadel,^b Severine Bellayer,^a
Jérôme Hosdez,^c Clément Vandingenen,^d Fadi Soubhie,^d Martial Belhache,^d Philippe Supiot,^a
and Ulrich Maschke^{*a}

a. Unité Matériaux et Transformations (UMET), UMR 8207–CNRS, University Lille, CNRS, INRAE, Centrale Lille, F-59000 Lille, France. E-mail: shagor.chowdhury@univ-lille.fr, ulrich.maschke@univ-lille.fr.

b. Institut Michel-Eugène Chevreul (IMEC)- FR 2638-CNRS, Univ. Lille, CNRS, INRAE, Centrale Lille, Univ. Artois, F-59000 Lille, France.

c. CNRS, Centrale Lille, UMR 9013 – LaMcube – Laboratoire de Mécanique, Multiphysique, Multiéchelle, University of Lille, 59000 Lille, France.

d. CRITT M2A, 62700 Bruay-la-Buissière, France.

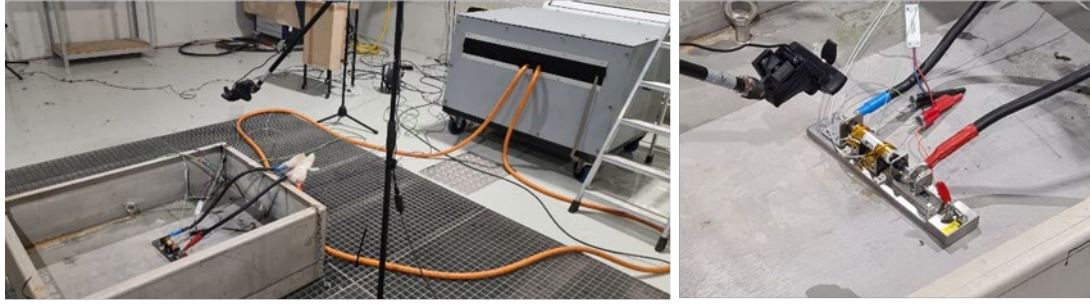


Figure S1. Digital photos of the installation in order to perform the external short circuit.

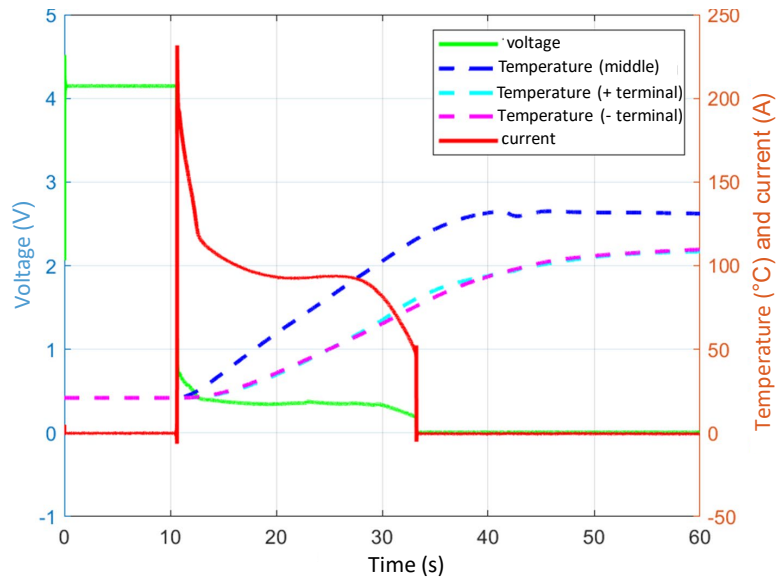


Figure S2. Evolution of voltage, current and temperature upon performing an external short circuit on a new cell.

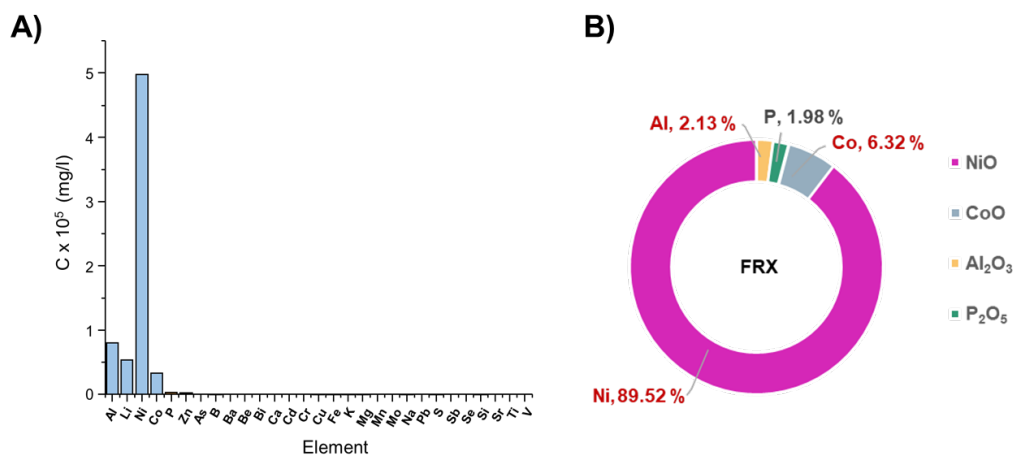


Figure S3. A) ICP-OES analysis of the cathode retrieved from pristine cell discharged to 0V. B) Results of X-ray fluorescence analysis of cathode electrode retrieved from pristine cell discharged to 0V.

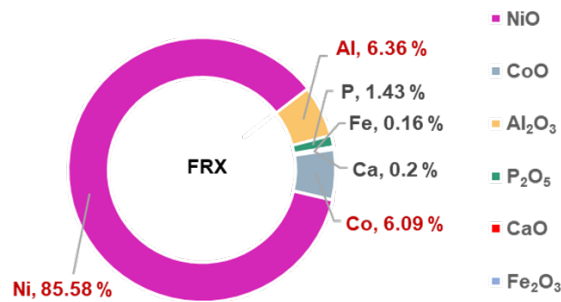


Figure S4. Results of X-ray fluorescence analysis of cathode retrieved from cell subjected to ESC conditions.

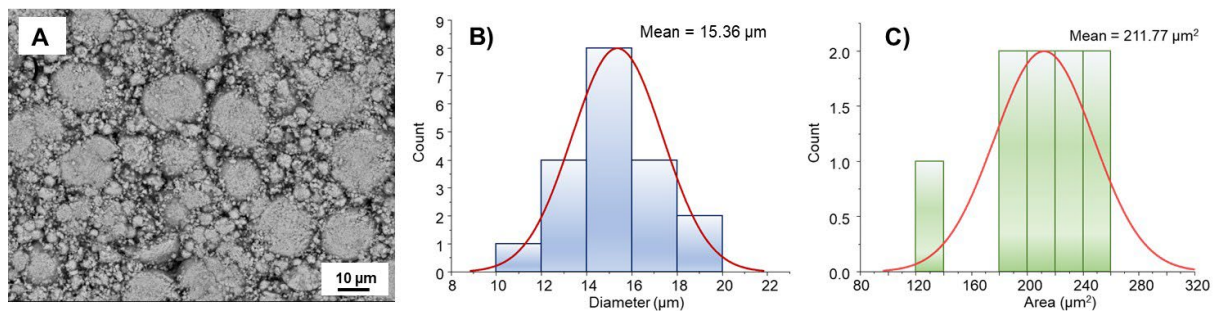


Figure S5. A) SEM image of the cathode retrieved from the pristine cell discharged to 0 V, B) statistical analysis of the cathode to determine the average diameter and (C) Statistical analysis of the cathode to determine area of the agglomerates.

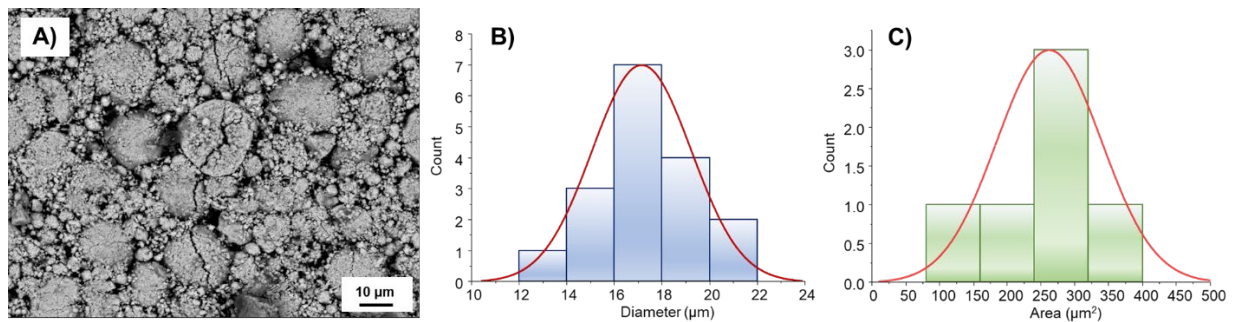


Figure S6. A) SEM image of the cathode retrieved from the ESC, B) statistical analysis of the corresponding cathode to determine the average diameter and (C) Statistical analysis of the cathode to determine area of the agglomerates.

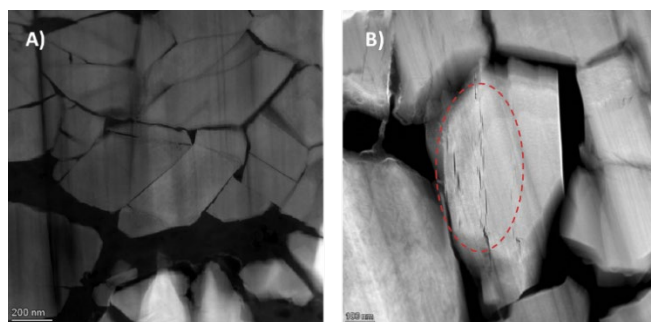
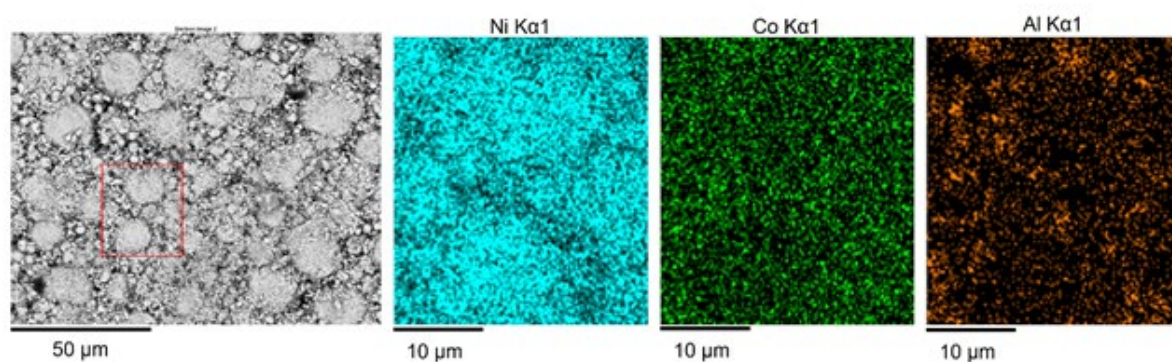


Figure S7. Representative HAADF-STEM images of the cathodes retrieved from: (A) the pristine cell discharged to 0 V and B) the ESC.

A)



B)

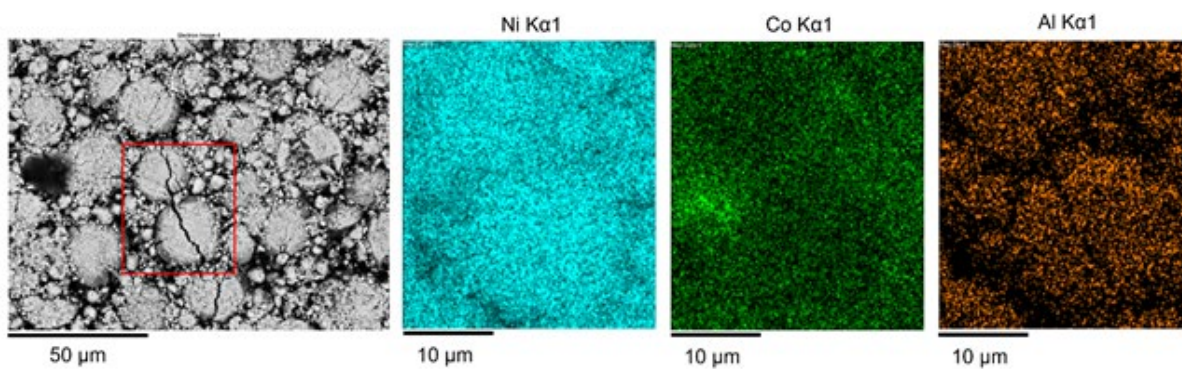


Figure S8. EDX maps of the cathode retrieved from A) pristine cell discharged to 0V, B) cell subjected to ESC conditions.

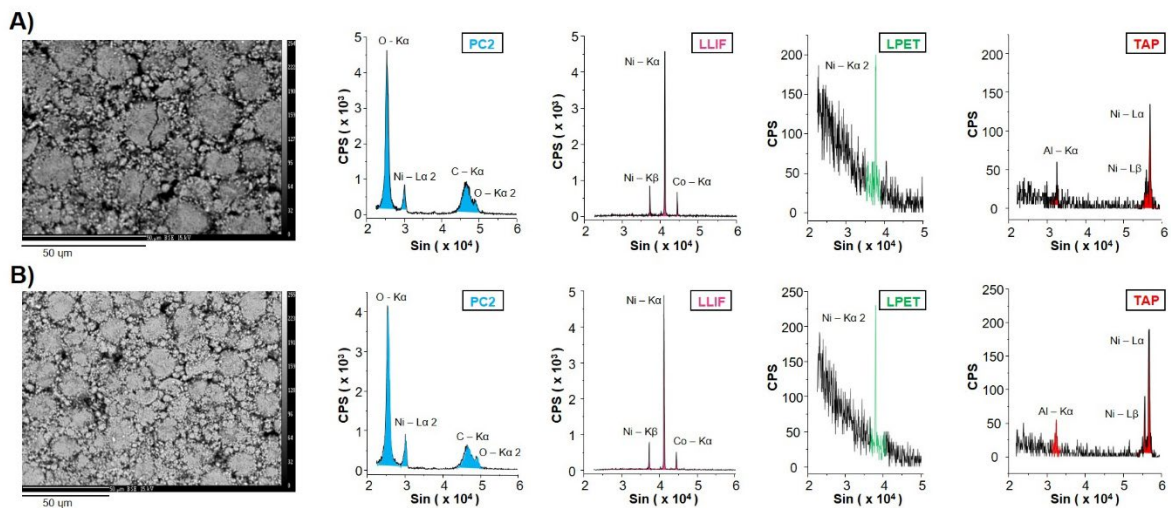


Figure S9. EPMA data of the cathode retrieved from A) pristine cell discharged to 0V, B) cell subjected to ESC conditions.

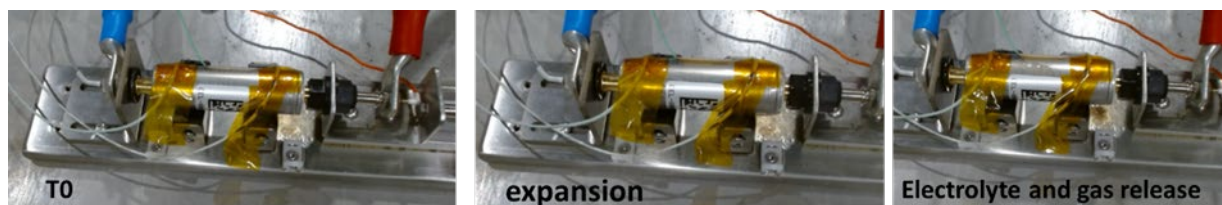
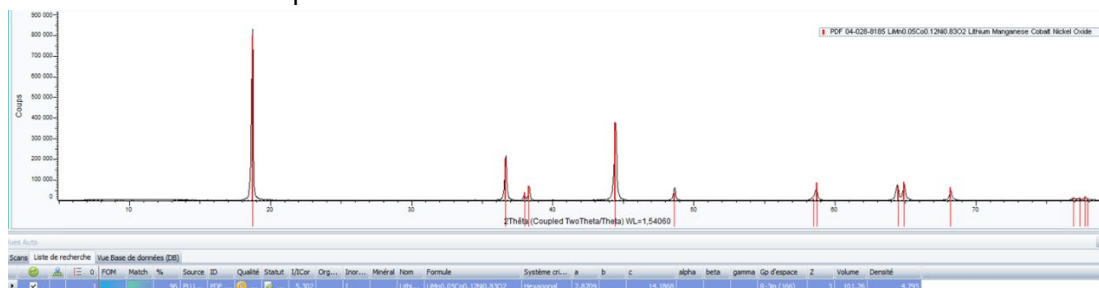


Figure S10. Images captured during short circuit process.

1) Cathode material from pristine cell



2) Cathode material from ESC cell

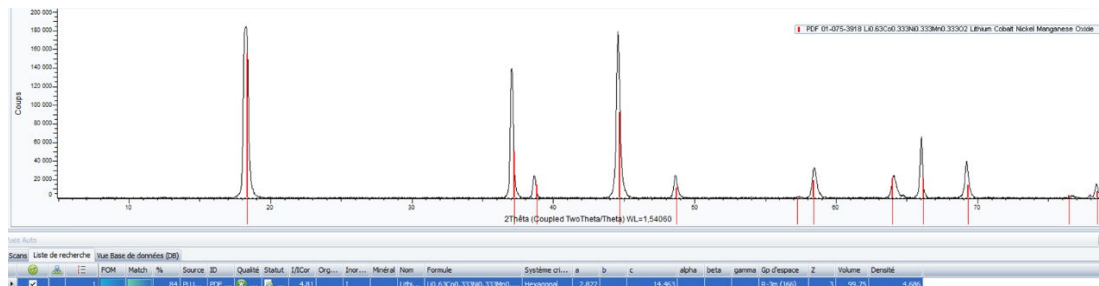
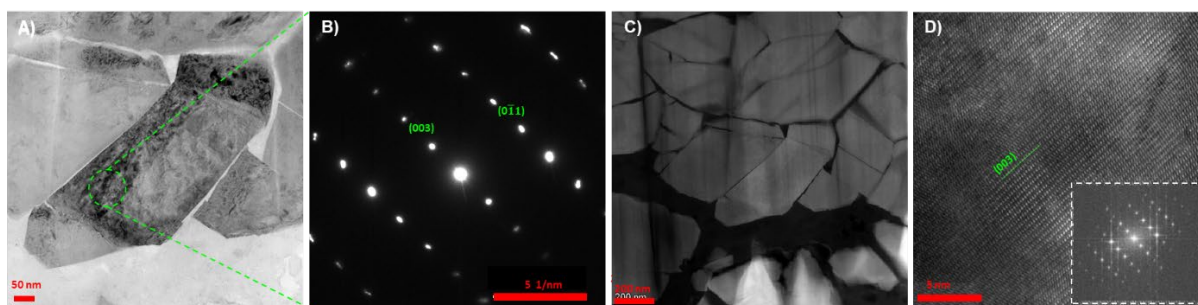
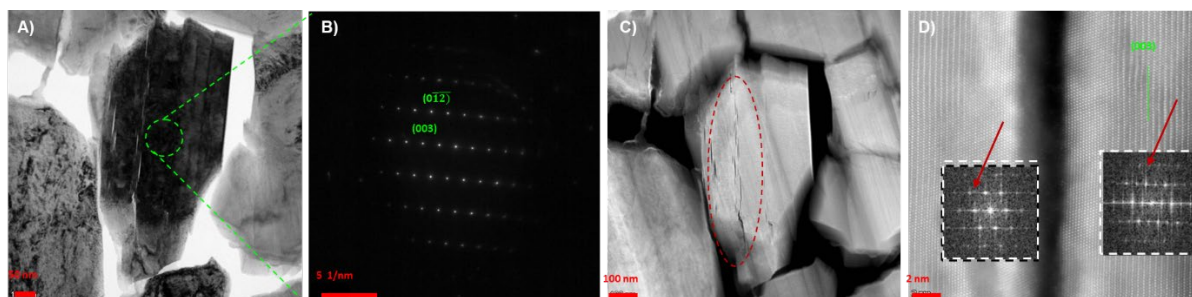


Figure S11. Screen shots obtained of the fitting data points obtained of the cathode materials



The measured distances correspond to $d_{(003)}=4.67 \text{ \AA}$

Figure S12. Representative images of the cathode retrieved from pristine cell discharged to 0V: (A) BF-TEM; (B) SAED pattern from the circled area along the [100] zone axis of NCA (indexed with space group $R\bar{3}m$); (C) HAADF-STEM; (D) High-resolution HAADF-STEM with FFT shown in the inset.



The measured distances correspond to $d_{(003)}=4.72 \text{ \AA}$

Figure S13. Representative images of the cathode retrieved from cell subjected to ESC conditions: (A) BF-TEM; (B) SAED pattern from the circled area along the [100] zone axis of NCA (indexed with space group $R\bar{3}m$); (C) HAADF-STEM; (D) High-resolution HAADF-STEM with FFT shown in the inset.

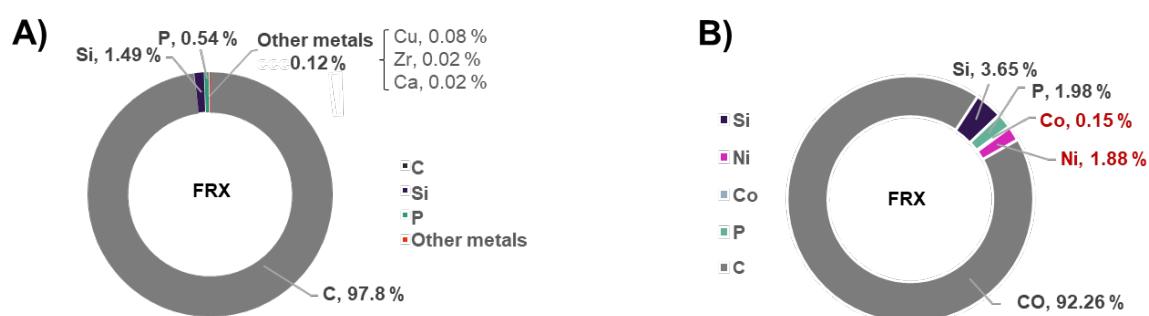


Figure S14. Results of X-ray fluorescence analysis of the anode retrieved from A) pristine cell discharged to 0V, B) cell subjected to ESC conditions.

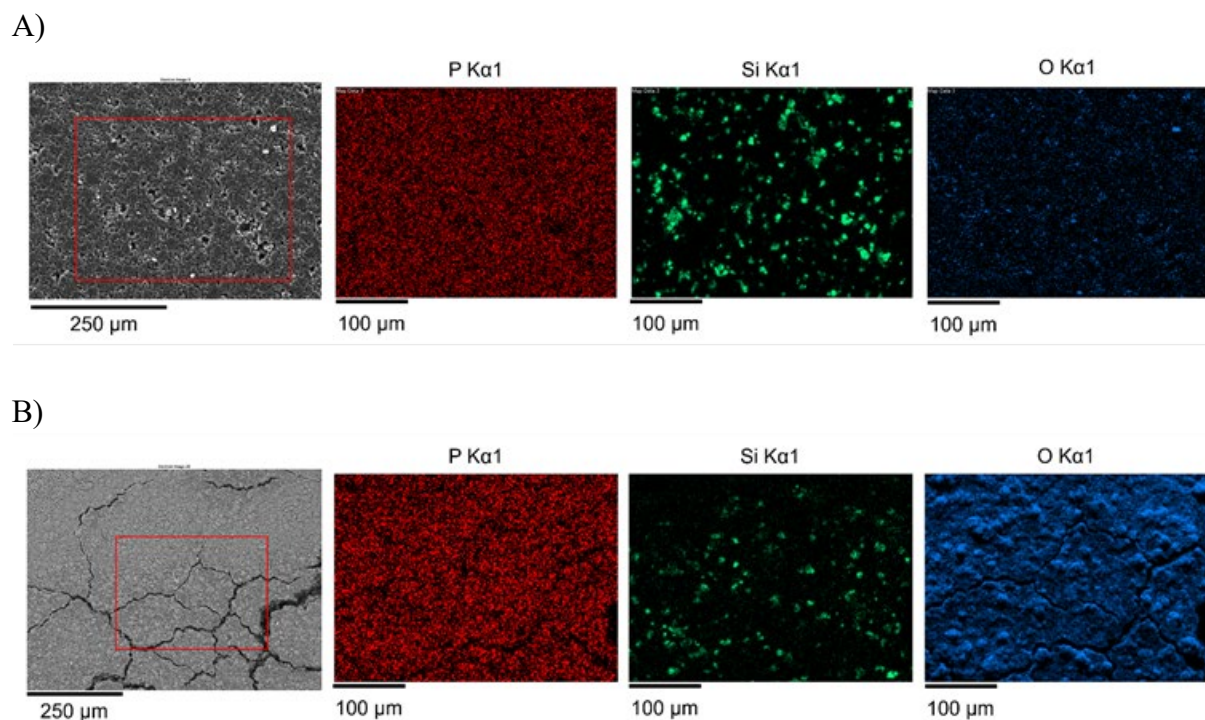


Figure S15. EDX mapping of the surface of the anode retrieved A) from pristine cell discharged to 0V and B) cell subjected to ESC conditions.

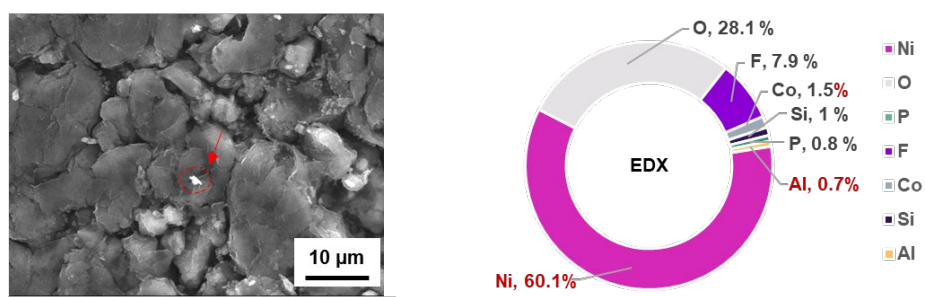


Figure S16. SEM micrographs and corresponding chemical composition analysis of the particle marked by a red arrow on the anode surface retrieved from the pristine cell discharged to 0V.

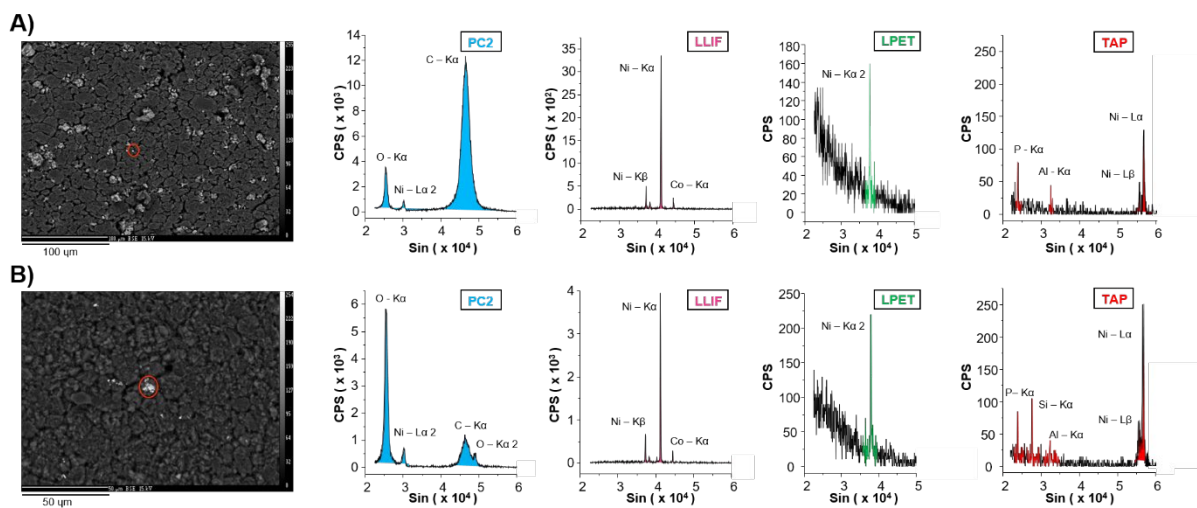


Figure S17. EPMA data of the anode retrieved from A) pristine cell discharged to 0V, B) cell subjected to ESC conditions.

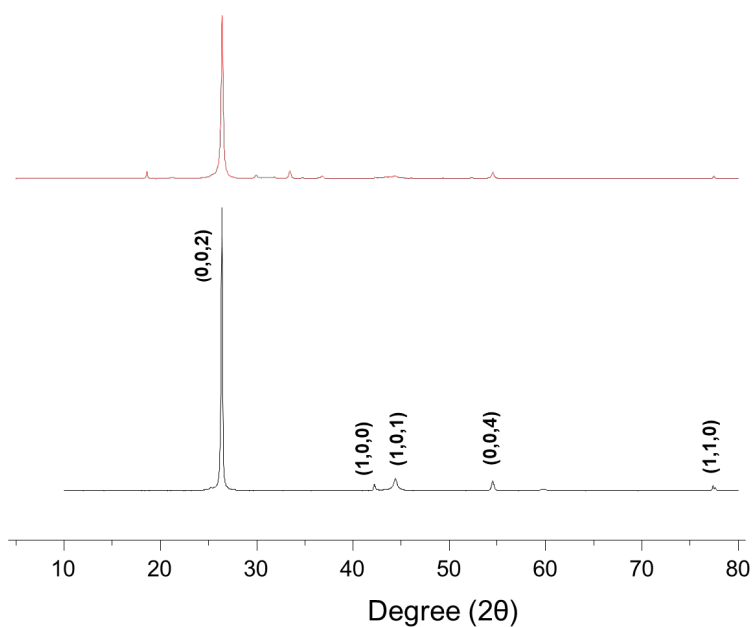
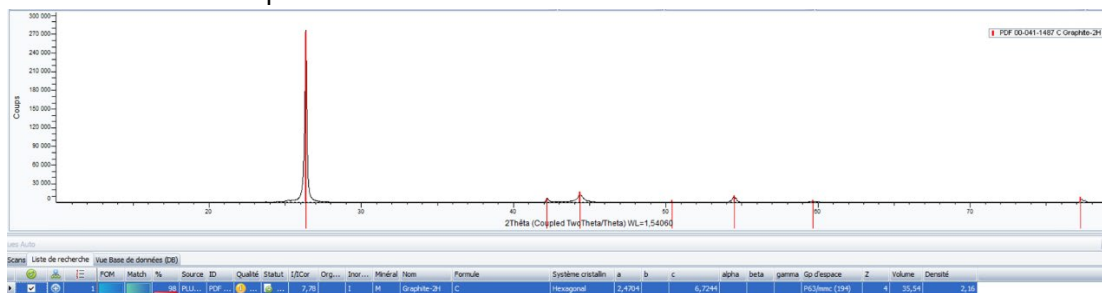


Figure S18. XRD patterns of the anode retrieved from pristine cell discharged to 0V (black) and from the cell subjected to ESC conditions (red).

1) Anode material from pristine cell



2) Anode material from ESC cell

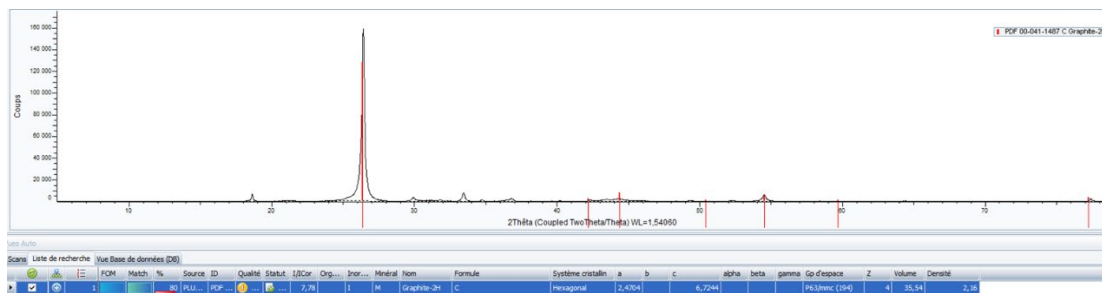


Figure S19. Screen shots obtained of the fitting data points obtained of the anode materials

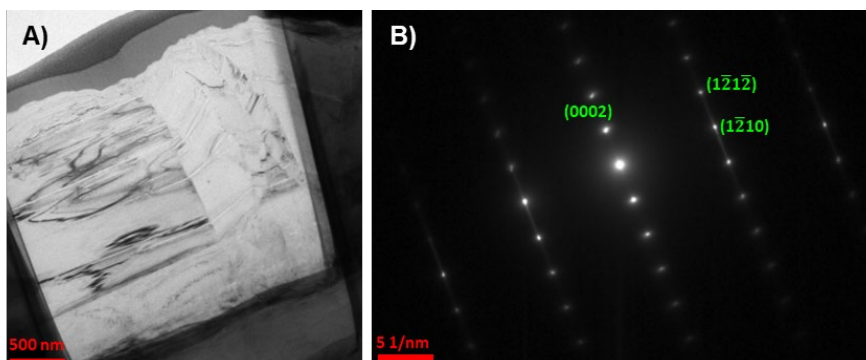


Figure S20. Representative images of the anode retrieved from pristine cell discharged to 0V: (A) BF-TEM; (B) SAED pattern from the circled area along the $[10\bar{1}0]$ zone axis of NCA (indexed with space group P63/mmc).

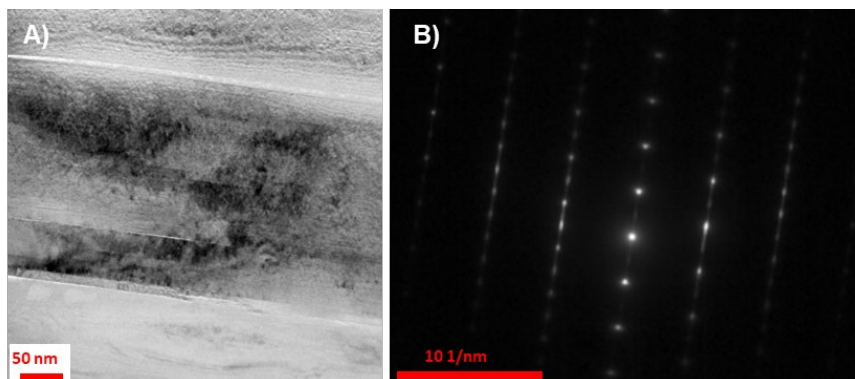


Figure S21. Representative images of the anode retrieved from ESC cell: (A) BF-TEM; (B) SAED pattern from the circled area along the $[10\bar{1}0]$ zone axis of NCA (indexed with space group P63/mmc).

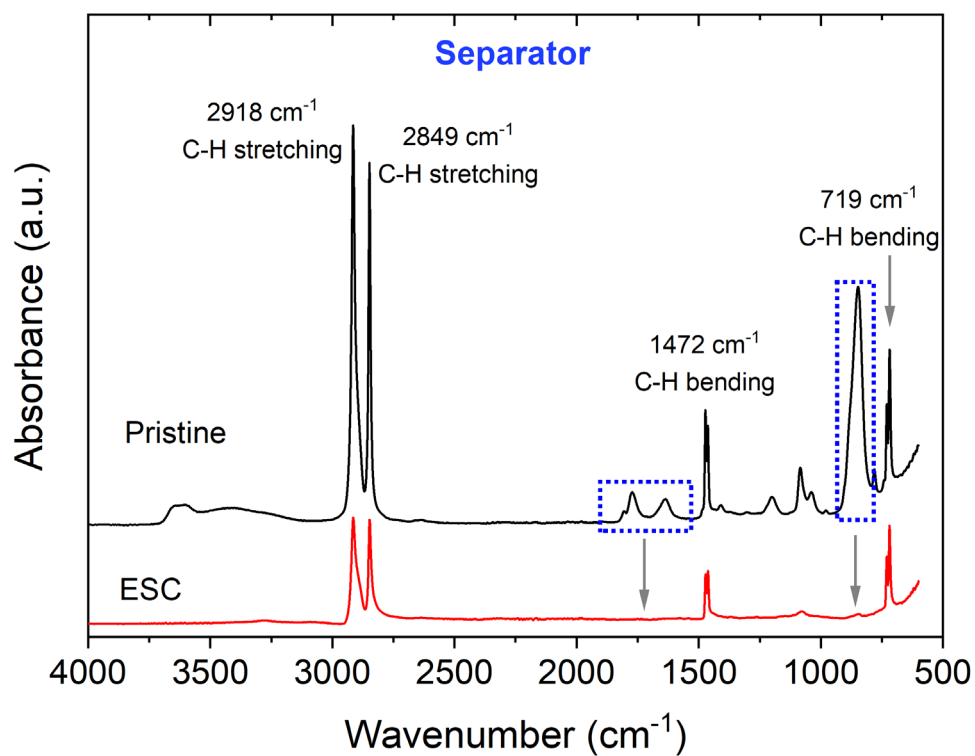


Figure S22. FTIR spectra of the separator material. The pristine cell was discharged to 0V.

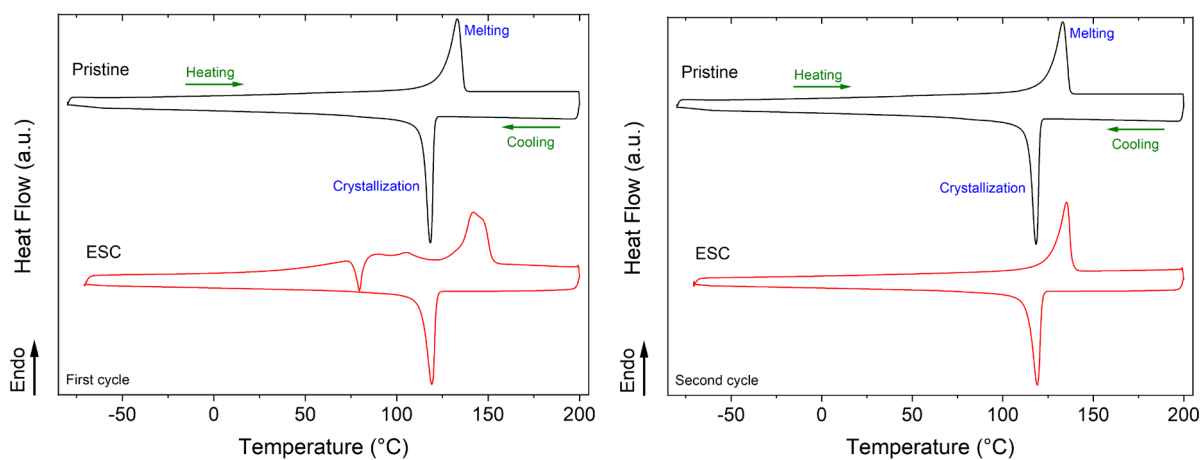


Figure S23. DSC thermograms of the separator material.

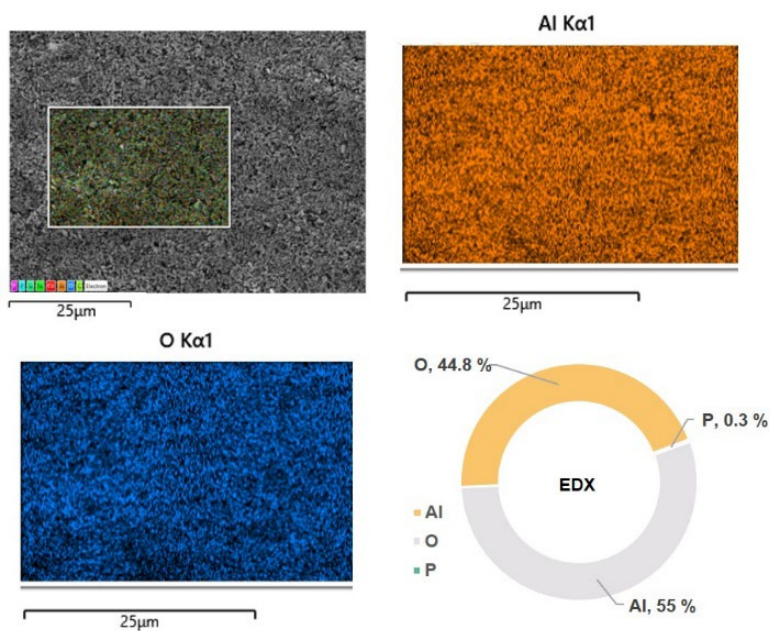


Figure S24. A) EDX map of the separator retrieved from the cell subjected to ESC conditions: side facing the cathode.

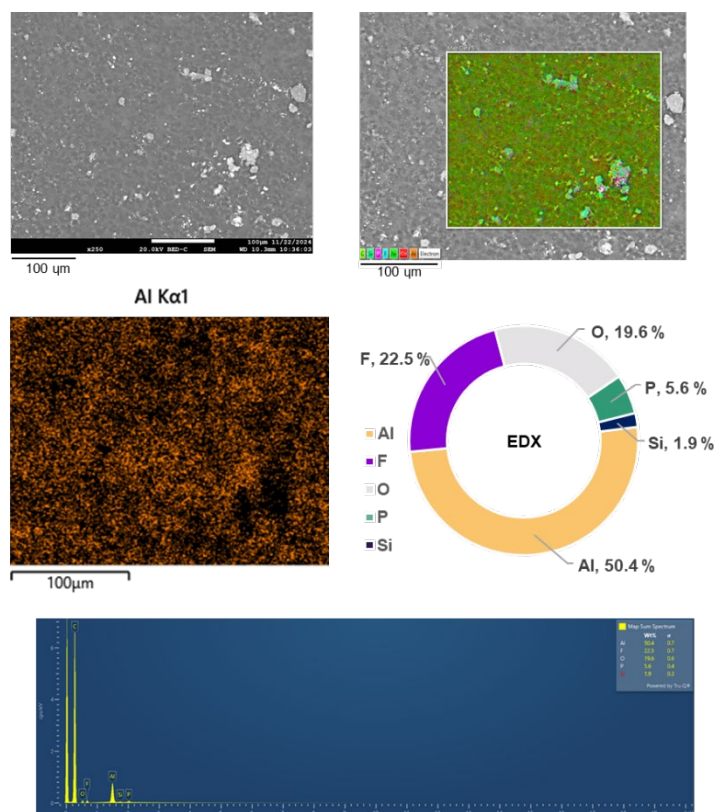
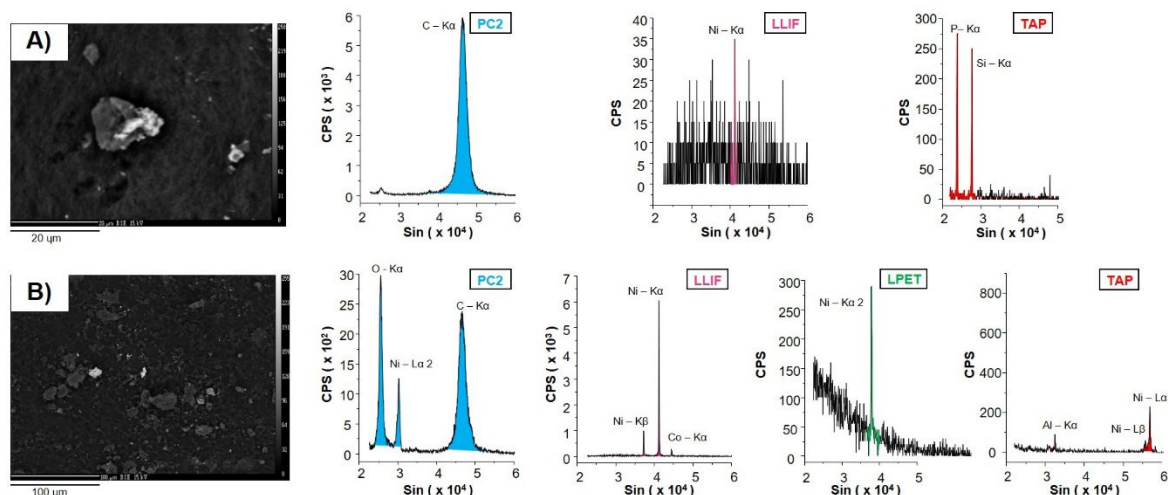
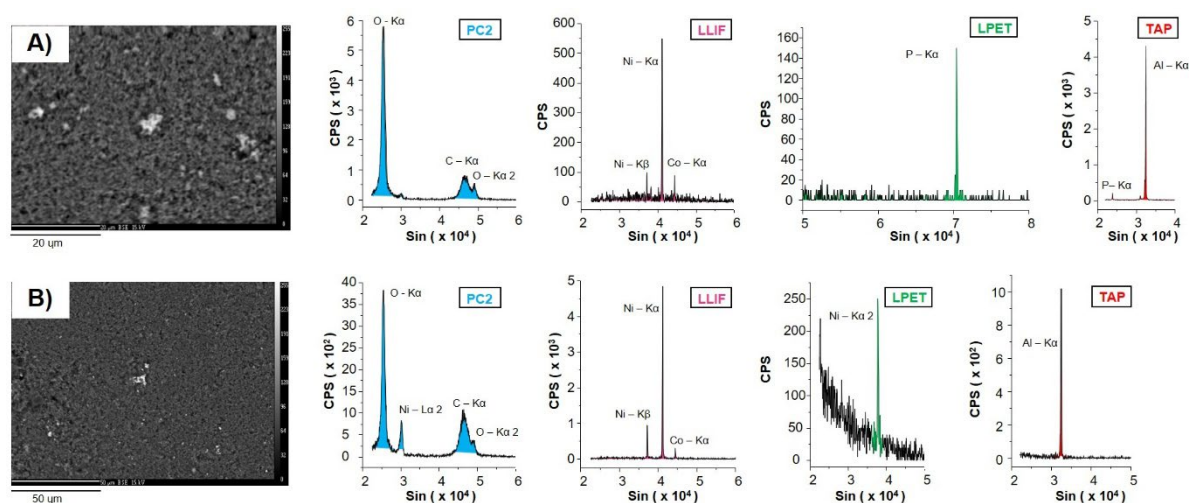


Figure S25. EDX map of the separator retrieved from the cell subjected to ESC conditions: side facing the anode.



Explanation: higher concentration of Ni and Co was observed in ESC anode compared to the anode retrieved from pristine cell.

Figure S26. EPMA data of the separator (side facing the anode) retrieved from the A) pristine cell discharged to 0V and B) cell subjected to ESC conditions.



Explanation: higher concentration of Ni and Co was observed in ESC anode compared to the anode retrieved from pristine cell.

Figure S27. EPMA data of the separator (side facing the cathode) retrieved from the A) pristine cell discharged to 0V and B) cell subjected to ESC conditions.

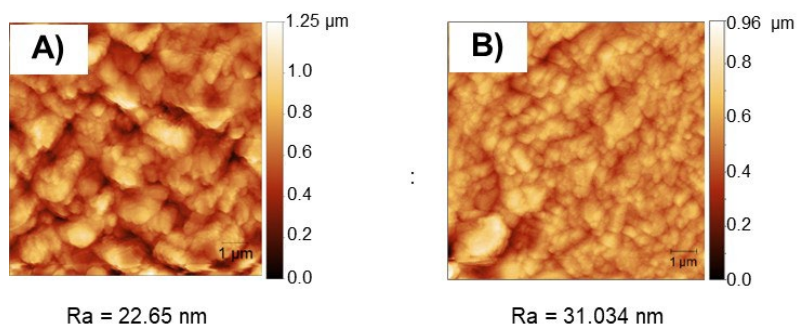


Figure S28. AFM height images of the separator (side facing the cathode) retrieved from the A) pristine cell discharged to 0V and B) cell subjected to ESC conditions

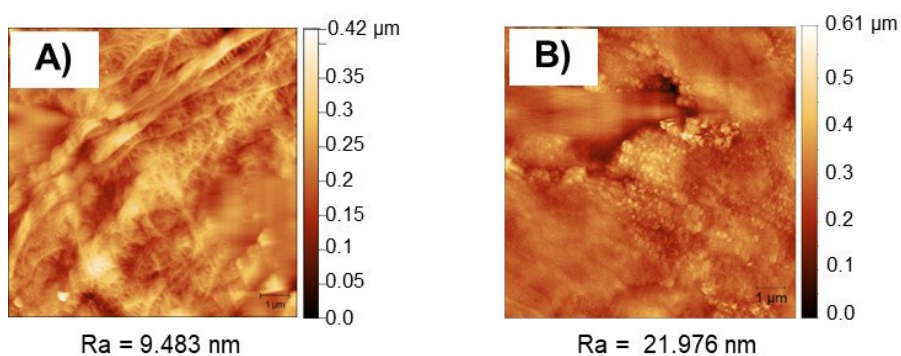


Figure S29. AFM height images of the separator (side facing the anode) retrieved from the A) pristine cell discharged to 0V and B) cell subjected to ESC conditions

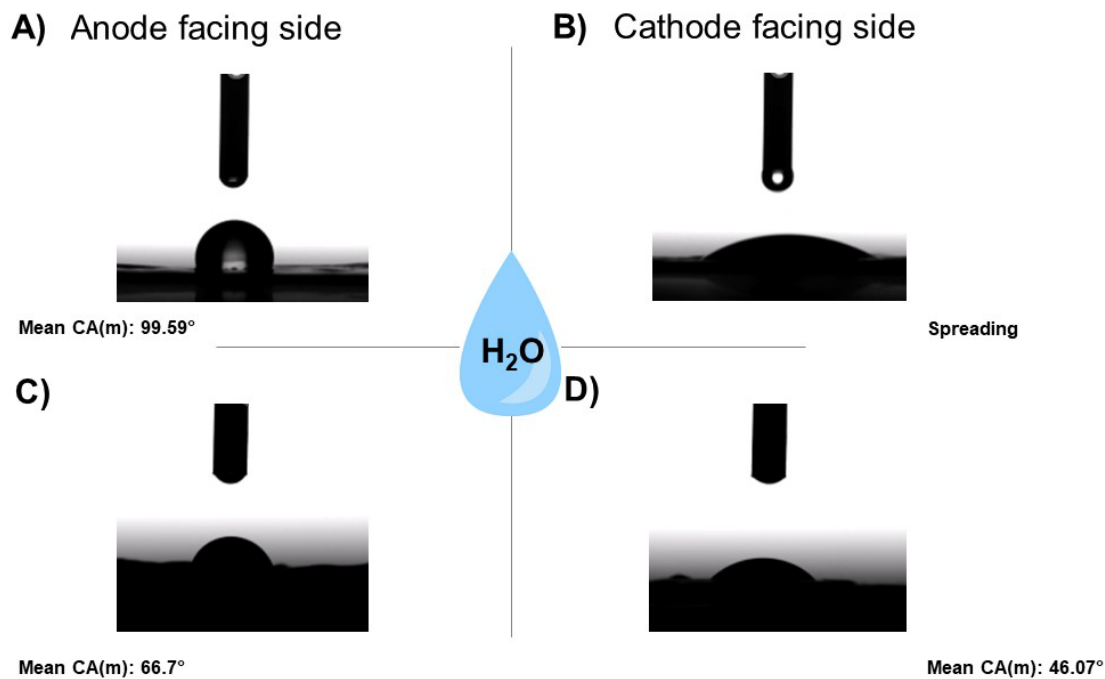


Figure S30. Contact angle measurements of the separators: A) side facing the anode from the pristine cell discharged to 0V, B) side facing the cathode from the pristine cell discharged to 0V, C) side facing the anode from the cell subjected to ESC conditions and D) side facing the cathode from the cell subjected to ESC conditions.

References:

1. Li, H.; Mo, Y.; Wang, L.; Wang, X., Feasibility of hydrophilic polyethylene separator for membrane bioreactor for wastewater treatment: Fouling behaviors and cleaning. *Water Cycle* **2023**, *4*, 79-86.